Supporting Information

Characterization of an Airborne Laser-Spark Ion Source for Ambient Mass Spectrometry

Andreas Bierstedt[†], Hendrik Kersten[‡], Reto Glaus[†], Igor Gornushkin[†], Ulrich Panne[†], Jens Riedel[*,†].

[†] Bundesanstalt für Materialforschung und -prüfung, BAM, Richard-Willstätter-Strasse 11, 12489, Berlin, Germany

[‡] University Wuppertal, Gaussstrasse 20, 42119 Wuppertal, Germany

[*] Corresponding author: Jens Riedel, E-mail: Jens.Riedel@bam.de, Tel.: +49 30 8104-1162, Fax: +49 30 8104-1167

Table of contents

Figure S-1. Schematic of the API HTOF mass spectrometer. S-3

Figure S-2. TPS (TOF Power Supply) software. S-4

Figure S-3. Reagent-ion spectrum (without gas) S-4

Figure S-4. Reagent-ion spectrum (compressed air) S-5

Figure S-5. Reagent-ion spectrum (dry nitrogen) S-5

Figure S-6. Reagent-ion spectrum (argon) S-5

Figure S-7. Reagent-ion signal stability over time. S-6

Figure S-8. Total ion chronogram of consecutive injections of *n*-butanol. S-6

Figure S-9. Spatially resolved analyte ionization yields S-7

Figure S-10. Flow-dependent reagent-ion formation (compressed air) S-8

Figure S-11. Flow-dependent reagent-ion formation (dry nitrogen) S-8

Figure S-12. Flow-dependent reagent-ion formation (argon) S-8

Figure S-13. Flow-dependent ionization yields of *n*-butanol and toluene. (compressed air) S-9

Figure S-14. Flow-dependent ionization yields of *n*-butanol and toluene. (dry nitrogen) S-9

Figure S-15. Flow-dependent ionization yields of *n*-butanol and toluene. (argon) S-9

Figure S-16. Relative abundance of methyl salicylate at different gas-phase concentrations. S-10

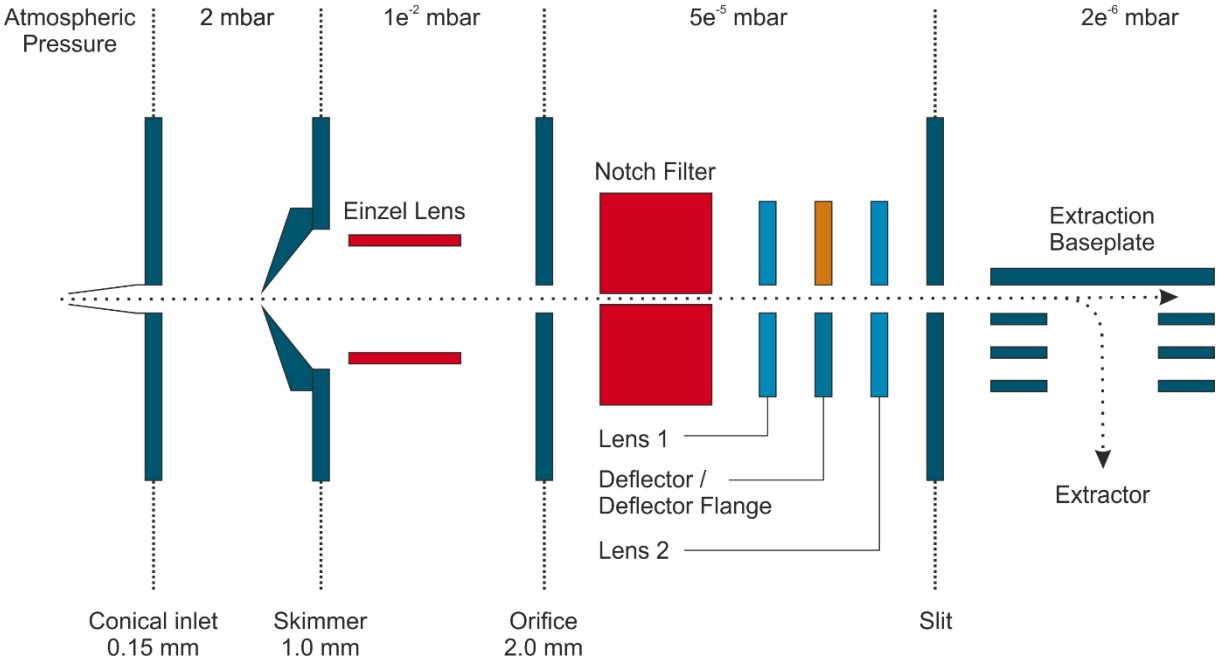

Figure S-1. Detailed schematic of the atmospheric pressure coupling interface of the modified API HTOF (TOFWERK AG, Thun, Switzerland) time-of-flight mass spectrometer. The instrument consists of differential pumping stages, equipped with ion guiding and focusing optics, which are sequentially passed. To ensure that the vacuum system can cope with the higher gas flux, the original pumping ensemble is backed up with an additional dry scroll vacuum pump (Varian TriScroll 600, Varian Inc. Vacuum Technologies, Lexington, MA, USA) in the first pumping stage and a rotary vane pump (Uno 30M, Pfeiffer Vacuum GmbH, Aßlar, Germany) as the forepump for a Flow 270 3P turbomolecular pump (Pfeiffer Vacuum GmbH, Aßlar, Germany). Transmission of ions generated in the reaction zone into the first pumping stage of the mass spectrometer, is achieved fluid-dynamically using a home-built conical inlet. For its design, the former inlet system, consisting of a metal plate with a central orifice of 0.3 mm in diameter, was extended by a commercially available airbrush nozzle (Harder & Steenbeck, Norderstedt, Germany). At the inlet towards atmospheric pressure, the inner diameter of this skimmer is 150 µm and increases linearly to 4 mm towards the vacuum system of the mass spectrometer, at a total length of 15 mm. The inlet is held at room temperature. Application of independent voltages to the inlet is possible. However, highest signal intensities for the LIP-TOF-MS set-up was achieved, when the electrode was floating between the neighboring potential fields. The second pumping stage is equipped with a skimmer (i.d. 1 mm), einzel lens combination, followed by a skimmer (i.d. 2mm), notch filter combination, before the orthogonal drift zone. Throughout all experiments, the notch filter was not in use. Optimization of the individual ion optic settings is performed by using the background signal of the laser-spark ion source. The instrument was operated in single reflectron geometry using the positive ion mode. All spectra were integrated over an acquisition time of 15 s with an extraction rate of 12.5 kHz.

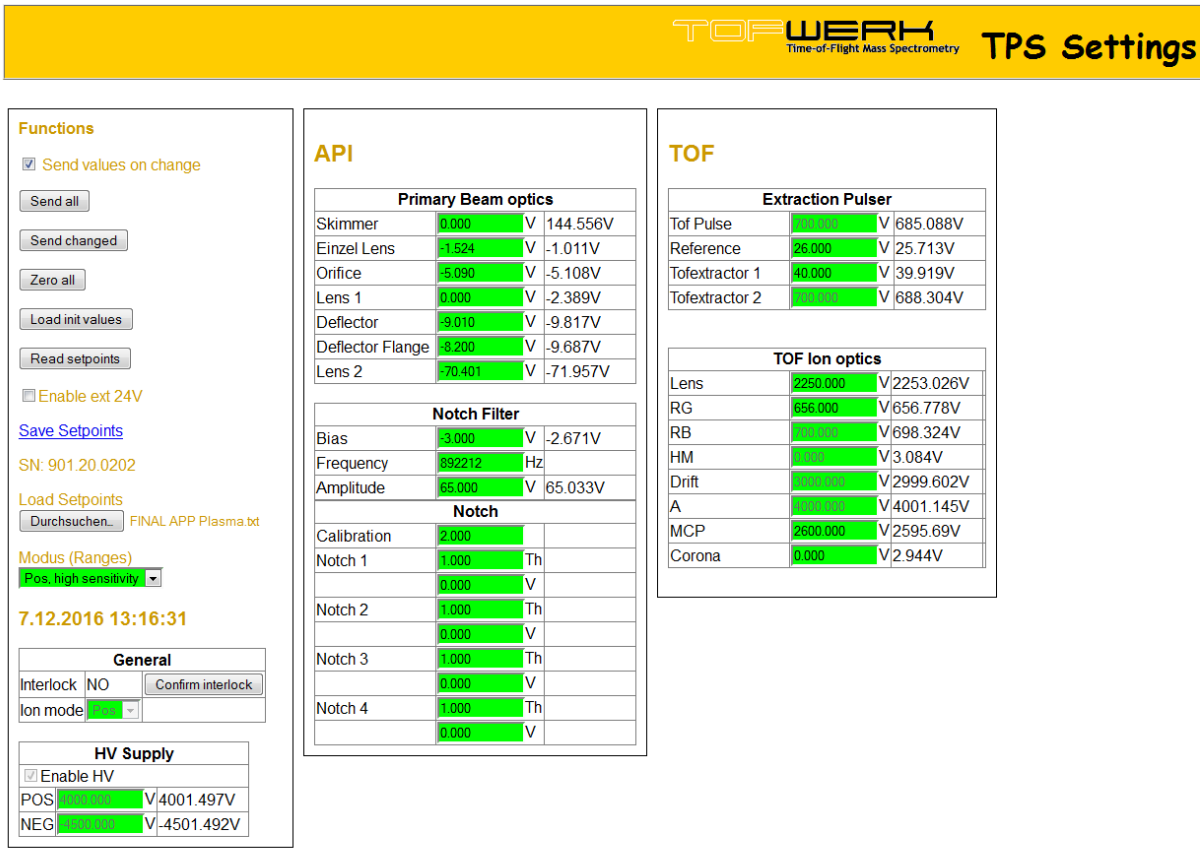

Figure S-2. TPS (TOF Power Supply) software used to control the applied voltages and ion optic settings of the time-of-flight instrument. The displayed settings were chosen for the laser-spark ion source in positive ion mode and single reflectron geometry.

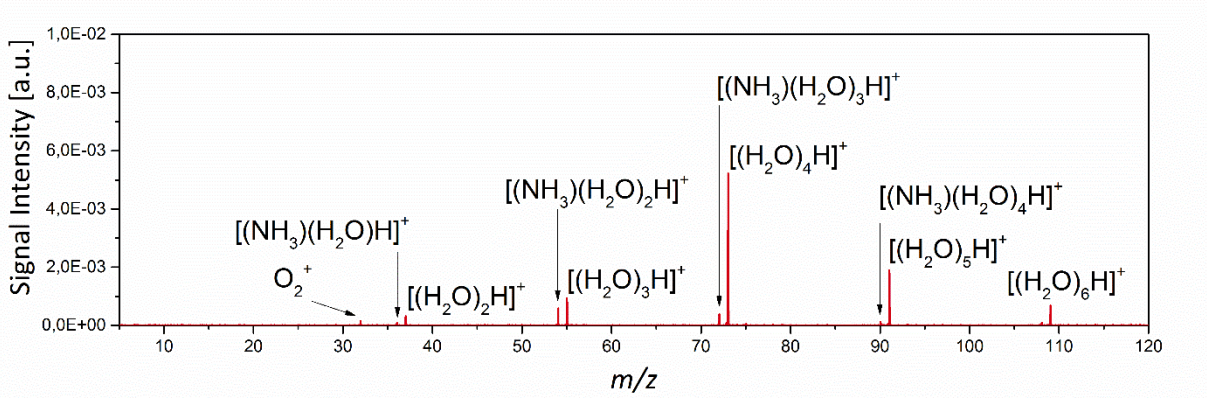

Figure S-3. Positive ions produced out of ambient air, using the laser-spark ion source. A carrier gas stream was not applied.

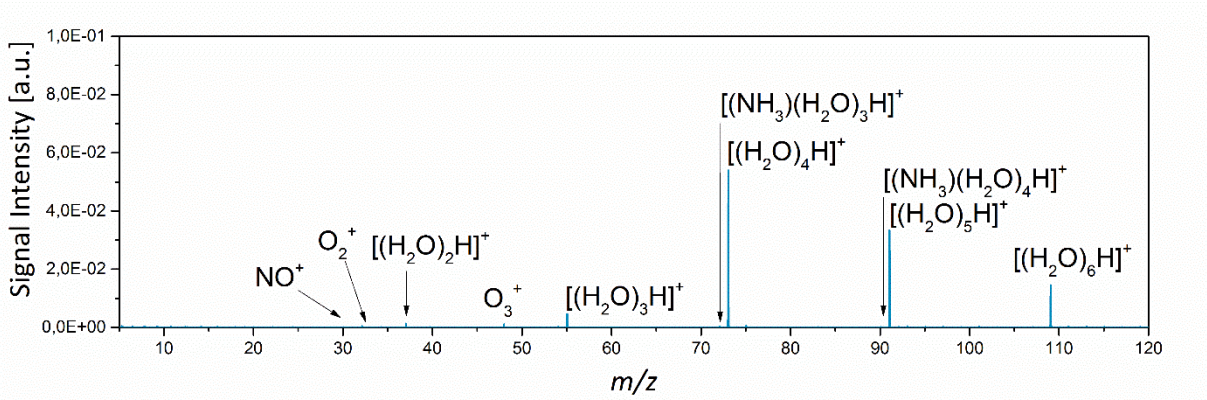

Figure S-4. Positive ions produced out of ambient air, using the laser-spark ion source. Compressed air (0.5 L/min) was used to replenish the late plasma zone.

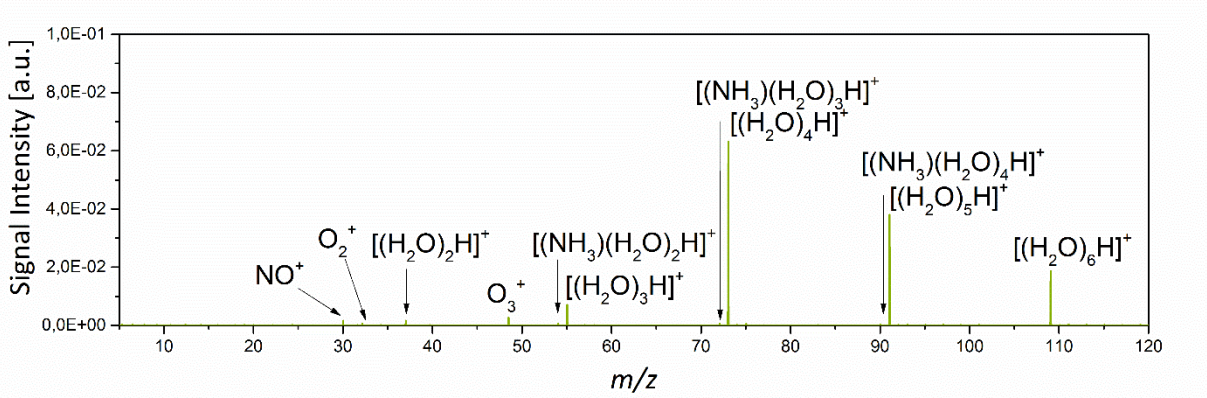

Figure S-5. Positive ions produced out of ambient air, using the laser-spark ion source. Dry nitrogen (0.5 L/min) was used to replenish the late plasma zone.

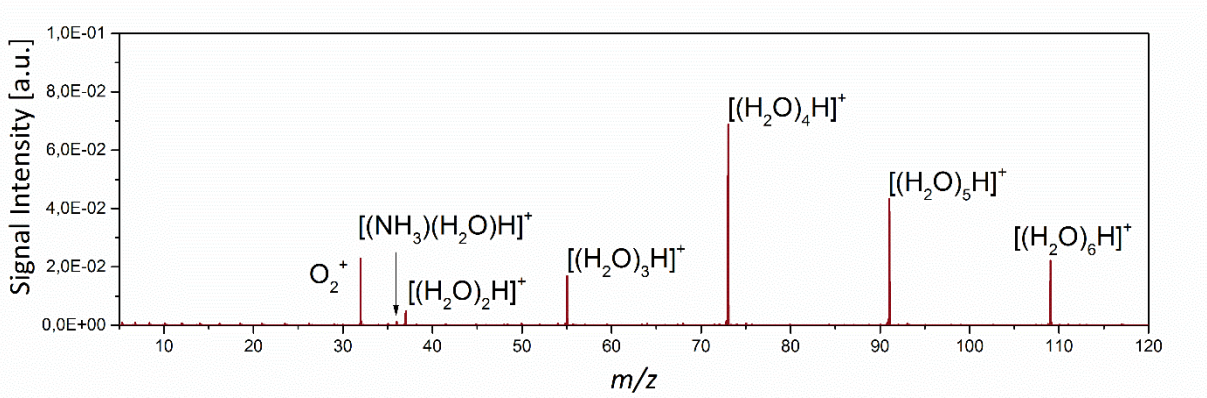

Figure S-6. Positive ions produced out of ambient air, using the laser-spark ion source. Argon (0.5 L/min) was used to replenish the late plasma zone.

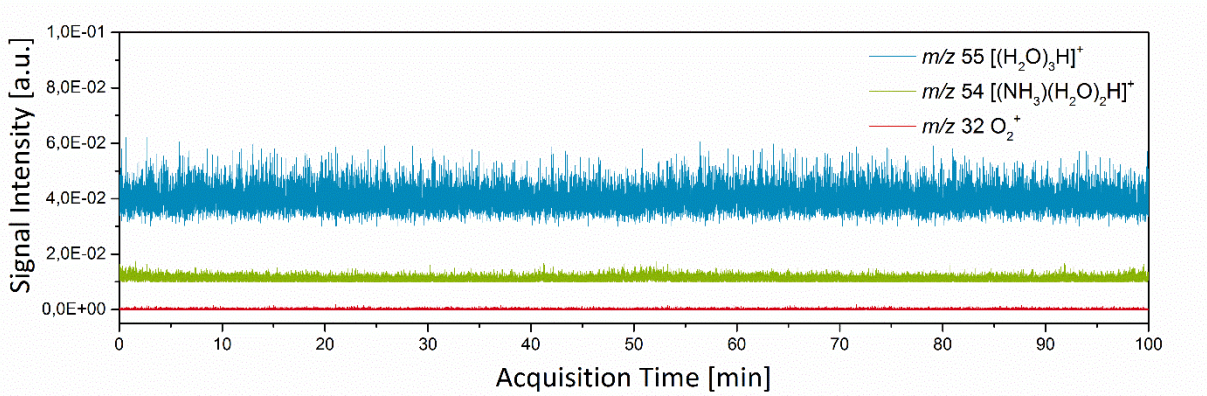

Figure S-7. Reagent-ion signal stability over time. Extracted total ion chronograms of *m/z* 55 $[(H_2O)_3H]^+$, *m/z* 54 $[(NH_3)(H_2O)_2H]^+$ and *m/z* 32 O_2^+, recorded over a timescale of 100 minutes, are shown. The ion source was ignited in the open lab environment without the use of a replenishing gas stream.

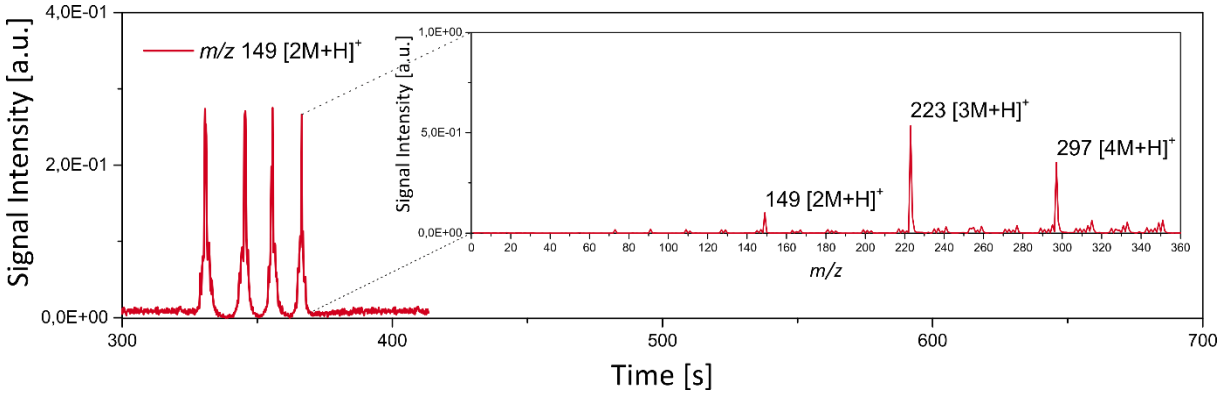

Figure S-8. Total ion chronogram of consecutive injections of *n*-butanol (10 ppm, v/v). The inset depicts the corresponding mass spectrum.

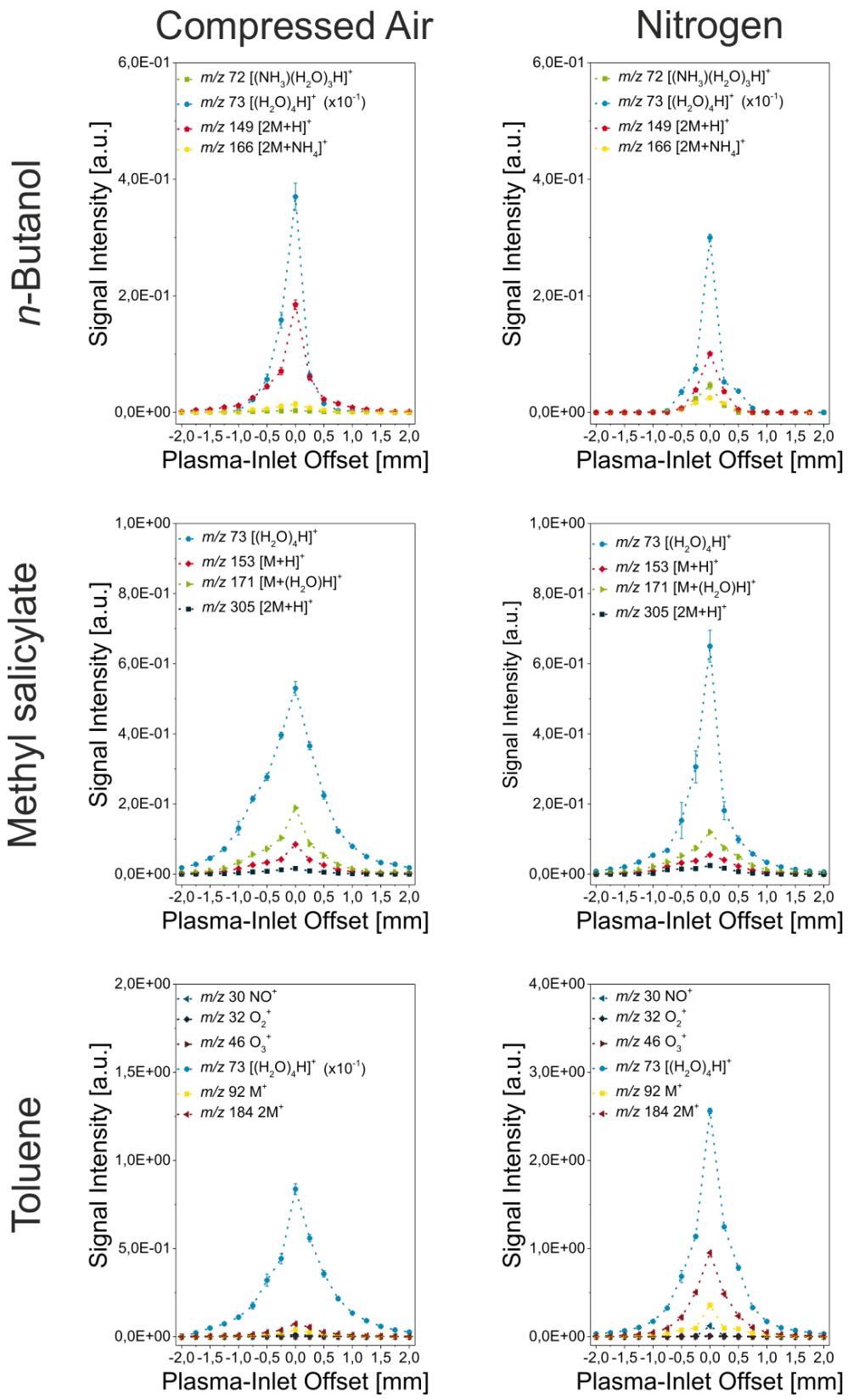

Figure S-9. Spatially resolved ionization yields of *n*-butanol, methyl salicylate and toluene (10 ppm, v/v, respectively). Introduction into the reactive zone was achieved via a carrier gas stream (2.0 L/min, compressed air or dry nitrogen). Please note the applied magnification factors.

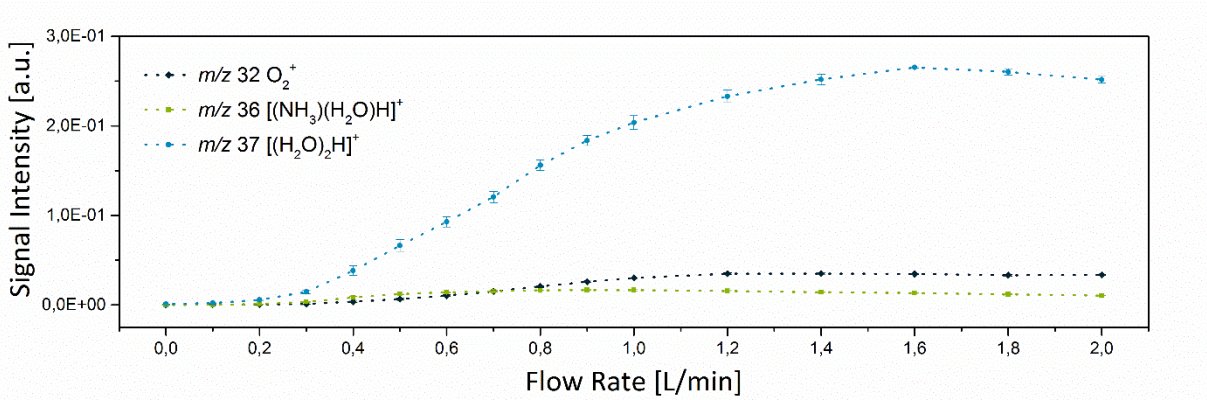

Figure S-10. Flow-dependent reagent-ion formation of the airborne laser-spark. An adjustable gas stream of compressed air was applied to regenerate the plasma center. Each data point depicts the sum of 400 subsequent mass spectra, acquired over 60 s.

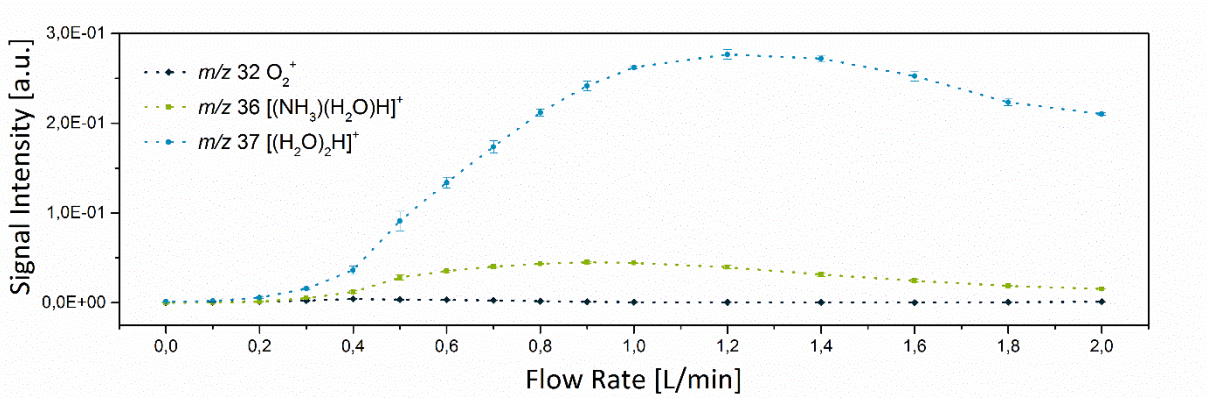

Figure S-11. Flow-dependent reagent-ion formation of the airborne laser-spark. An adjustable gas stream of dry nitrogen was applied to regenerate the plasma center. Each data point depicts the sum of 400 subsequent mass spectra, acquired over 60 s.

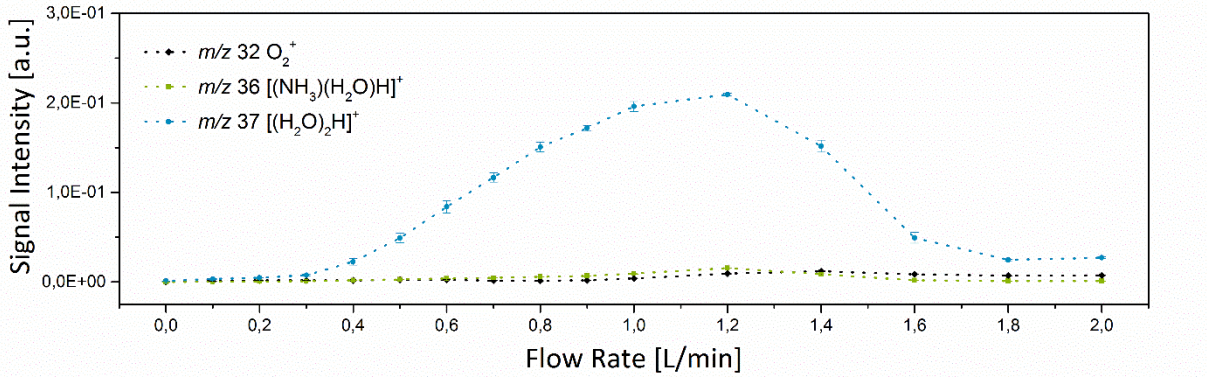

Figure S-12. Flow-dependent reagent-ion formation of the airborne laser-spark. An adjustable gas stream of argon was applied to regenerate the plasma center. Each data point depicts the sum of 400 subsequent mass spectra, acquired over 60 s.

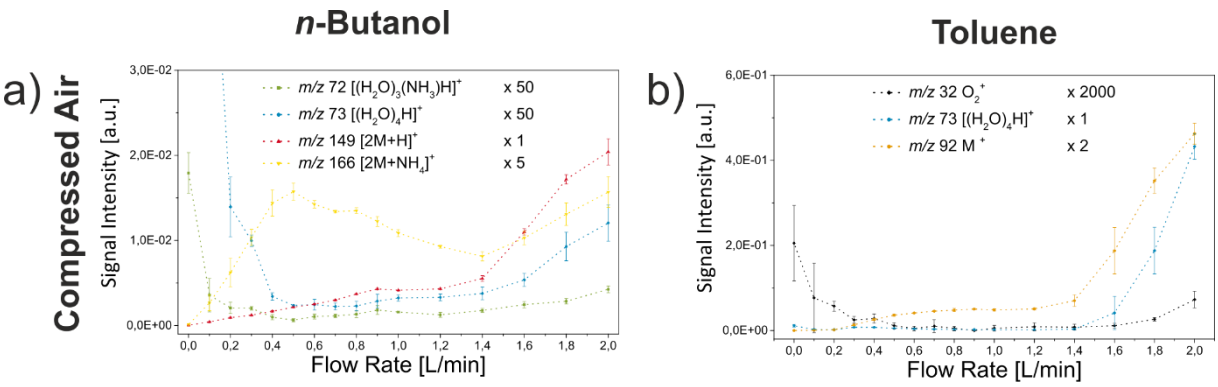

Figure S-13. Detailed flow-dependent ionization yields of *n*-butanol and toluene. A carrier gas stream of compressed air was applied. Magnification factors are arbitrary and for visualization purposes only.

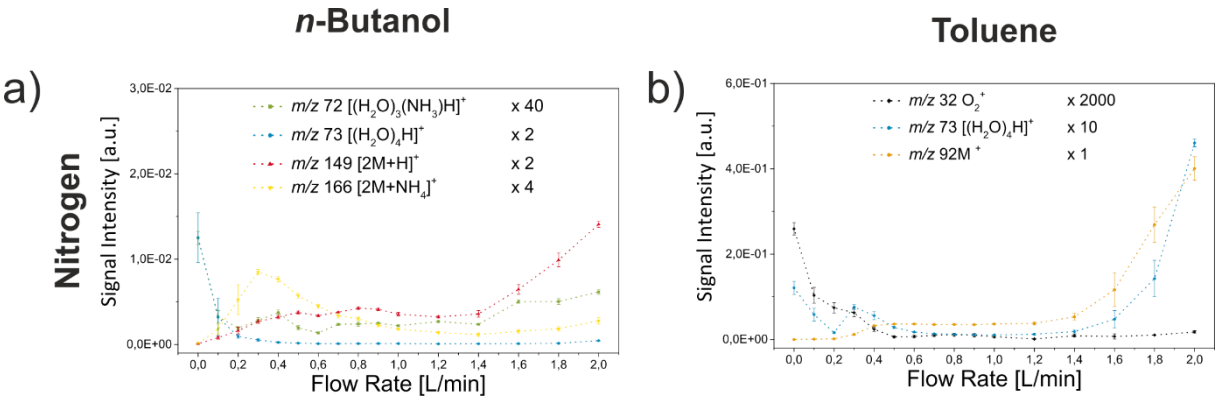

Figure S-14. Detailed flow-dependent ionization yields of *n*-butanol and toluene. A carrier gas stream of dry nitrogen was applied. Magnification factors are arbitrary and for visualization purposes only.

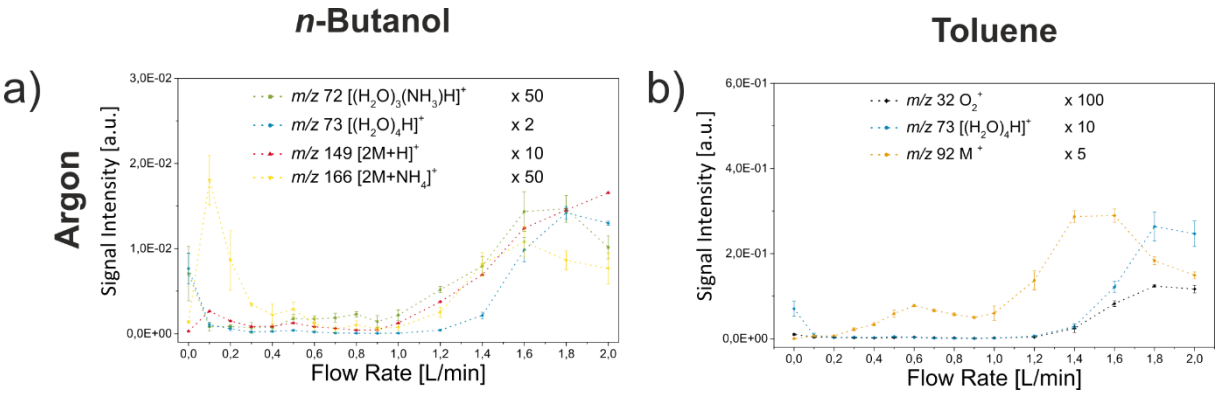

Figure S-15. Detailed flow-dependent ionization yields of *n*-butanol and toluene. A carrier gas stream of argon was applied. Magnification factors are arbitrary and for visualization purposes only.

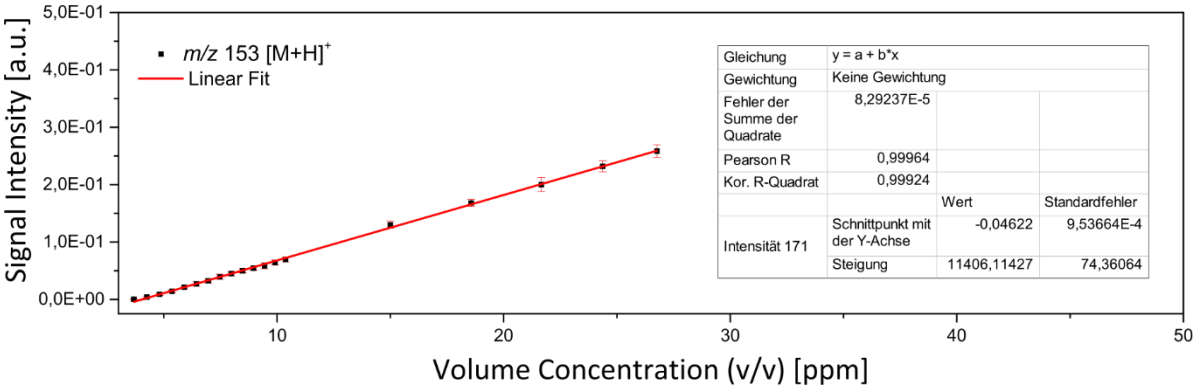

Figure S-16. Relative abundance of the protonated methyl salicylate monomer (*m/z* 153) at different gas-phase concentrations.